FABRICATION OF ACTIVE THIN FILMS FOR VIBRATION DAMPING IN MEMS DEVICES FOR THE NEXT GENERATION ARMY MUNITION SYSTEMS

E. Ngo*, W. D. Nothwang, M.W. Cole, C. Hubbard and G. Hirsch
U. S. Army Research Laboratory, WMRD
Weapons and Materials Research Directorate
Aberdeen Proving Ground, MD 21005

K.P. Mohanchandra and G. P. Carman
Mechanical & Aerospace Engineering Department,
University California at Los Angeles
Los Angeles, CA 90095-1361

ABSTRACT

This research combined continuum mechanics modeling, materials design, materials fabrication/processing, and experimental testing/characterization to promote a materials solution for passive damping of undesirable extrinsic vibrations in microelectromechanical-systems-based devices. Shape memory alloy, nickel titanium (NiTi) thin films were deposited by an in-situ reactive DC magnetron sputtering process and piezoelectric, barium strontium titanate ($Ba_{0.80}Sr_{0.20}TiO_3$) were fabricated using pulsed laser deposition and metal organic solution deposition techniques. These films were integrated as a bi-layer structure on *n*+ platinum silicon substrates to form a vibration-damping pedestal module known as "active materials". The optimized post deposition annealing temperatures for the shape memory alloy and piezoelectric thin films were determined to be 500 and 750 ^oC, respectively. Crystalline, pinhole-free, and crack-free films of 250-400 nm thickness were fabricated. The surface roughness of the films was around 2.2 nm with average grain size of approximately 50 nm. Cross-sectional microscopy affirmed the dense and uniform microstructure. The bilayer pedestal design concept offers a solution for passive damping.

1. INTRODUCTION

The development and potential fielding of the U.S. Army's Future Force (FF) next generation of smart missiles/munitions platforms (e.g., compact kinetic energy missile, smart cargo artillery, medium caliber munitions, etc.) is impeded by the inability to satisfy the FF performance standards for the precision and control of "target-hit interactions." This performance shortfall centers on the thesis that these FF munitions currently suffer from severe inaccuracies caused by a critical failure of the microelectromechanical-systems (MEMS) inertial measurement unit (IMU), i.e., angular rate sensor (ARS). The IMU is vulnerable to failure due to the harsh extrinsic vibration environment. The "extrinsic vibration" (harsh environment generated from launch and /or high-G in-flight forces) causes an out-of-plane motion or false angular rate signal to be generated. Since the MEMS-derived positional data is essential for the projectiles guidance/navigation, this false, vibration-derived angular rate signal causes the projectile to miss its designated target. Thus, reduction of susceptibility of the MEMS ARS to the adverse extrinsic vibrations must be addressed to ensure the accuracy of positional performance (i.e., ensure target-hit success) for such gun launched projectiles (Cole et al, 2003). Traditional vibration damping materials, e.g., viscoelastics, have a very high material dispersion coefficient, tan δ. Unfortunately, viscoelastics have a very low material stiffness, which limits the amount of energy that can be damped (Chaplya P. M., et al, 2002; Wollman. J. et al, 2003). Material stiffness is a function of temperature for most materials, but in viscoelastics the

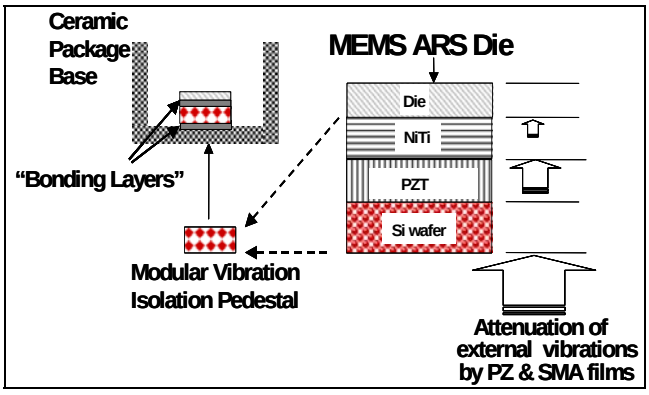

Figure 1. Schematic of a vibration control pedestal with a shape memory alloy and piezoelectric thin film bi-layer stack for passive damping for MEMS-based devices.

Report Documentation Page

Form Approved
OMB No. 0704-0188

1. REPORT DATE	2. REPORT TYPE	3. DATES COVERED
00 DEC 2004	**N/A**	**-**

4. TITLE AND SUBTITLE	5a. CONTRACT NUMBER
Fabrication Of Active Thin Films For Vibration Damping In Mems Devices For The Next Generation Army Munition Systems	5b. GRANT NUMBER
	5c. PROGRAM ELEMENT NUMBER
6. AUTHOR(S)	5d. PROJECT NUMBER
	5e. TASK NUMBER
	5f. WORK UNIT NUMBER
7. PERFORMING ORGANIZATION NAME(S) AND ADDRESS(ES) **U. S. Army Research Laboratory, WMRD Weapons and Materials Research Directorate Aberdeen Proving Ground, MD 21005; Mechanical & Aerospace Engineering Department, University California at Los Angeles Los Angeles, CA 90095-1361**	8. PERFORMING ORGANIZATION REPORT NUMBER
9. SPONSORING/MONITORING AGENCY NAME(S) AND ADDRESS(ES)	10. SPONSOR/MONITOR'S ACRONYM(S)
	11. SPONSOR/MONITOR'S REPORT NUMBER(S)

12. DISTRIBUTION/AVAILABILITY STATEMENT
Approved for public release, distribution unlimited

13. SUPPLEMENTARY NOTES
See also ADM001736, Proceedings for the Army Science Conference (24th) Held on 29 November - 2 December 2005 in Orlando, Florida. , The original document contains color images.

14. ABSTRACT

15. SUBJECT TERMS

16. SECURITY CLASSIFICATION OF:			17. LIMITATION OF ABSTRACT	18. NUMBER OF PAGES	19a. NAME OF RESPONSIBLE PERSON
a. REPORT	b. ABSTRACT	c. THIS PAGE			
unclassified	**unclassified**	**unclassified**	**UU**	**21**	

dependency is extreme, limiting their viability to a very narrow temperature range.

In this work, a design concept for a "vibration control pedestal" which consists of "active materials"; [i.e., shape memory alloy (SMA) and a piezoelectric thin film bilayer stack (Figure 1)] is explored. In the design concept, a silicon wafer supporting the bilayer active thin film stack is sandwiched between the die and device ceramic package. Using a continuum mechanics calculation to model the longitudinal vibration modes within the thin film pedestal, it was possible to examine a series of different materials. The pedestal was modeled as a multilayer material with distinct, but mathematically continuous, interfaces. The model indicates the ideal damping materials have a high stiffness and tan δ, and the materials should also be immune to harsh environments. Based on the modeling, thin film piezoelectric materials and shaped memory alloy metals

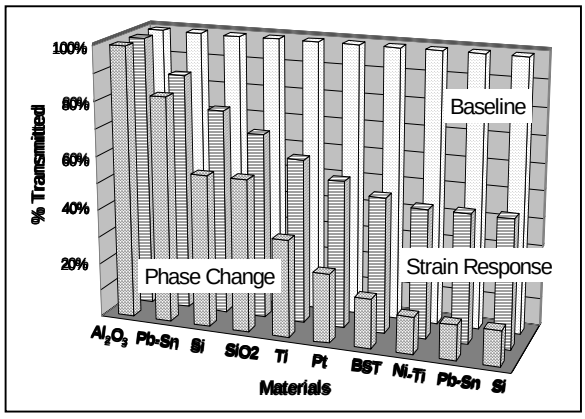

Figure 2. Vibration damping characteristics of various configurations of the pedestal design.

(Figure 2) offer enhanced material dispersion, relatively high stiffness and the ability to tune and optimize the performance over the desired environmental window.

2. EXPERIMENTAL

The fabrication of thin and thick films has been reported using many techniques, such as sol-gel, hydrothermal, electrophoretic, reactive partially ionized beam deposition, and metal organic chemical vapor deposition (Kamalasanan et al. 1991; Ngo et al., 2001; Morita et al., 2004; Singh P. K. et al 1995; Jeon et al., 1991). Each of these techniques offers some advantages as well as disadvantages, and may require high cost investment, a complicated apparatus and a complex set of deposition parameters. For this research, three different deposition methods and three approach pedestal configurations were evaluated. SMA, nickel titanium (NiTi) was deposited by a magnetron DC sputtering, and piezoelectric ($Ba_{0.80}Sr_{0.20}TiO_3$) thin films were deposited by two different methods, pulsed laser deposition (PLD) and metal organic solution deposition (MOSD).

For SMA, the NiTi films were deposited by DC magnetron sputtering system (1) directly on Si wafer as the base layer, as the second top layer of the pre-deposited, (2) un-annealed and (3) annealed piezoelectric $Ba_{0.80}$ $Sr_{0.20}TiO_3$ thin films. The sputtering system is an ultra high vacuum system with a load lock to decrease pump down time as well as eliminate contamination. Water and carbon dioxide are the main source of contamination (Mohanchandra K. P et al, 2002, Cole et al, 2000; Cole et al, 2001); therefore, a residual gas analyzer (RGA) was used to closely monitor contamination levels, prior to sputtering. A 3-inch DC magnetron gun was used for deposition. A substrate holder with a heater and rotation capability was used to in-situ anneal the film. NiTi target was obtained from Special Metals Inc., and then machined to the desired dimension. The target temperature during sputtering ramped up to 700°C. This high temperature was achieved by reducing the thermal paste, thereby producing a poor thermal contact between the target and the copper chill block. All films were deposited at a base pressure below 5 x 10^{-8} Torr, while argon pressure during sputtering was kept at 2 x 10^{-3} Torr. Substrate to target distance was kept at 4 cm and sputtering power was 300 Watts (Mohanchandra et al, 2002). The deposition rate at these conditions was approximately 0.76 nm/s. Deposited films were in-situ annealed by the substrate heater at 500 °C for 10 min prior to removal from the sputtering system. Figure 3 shows X-ray diffraction patterns of a well crystallized NiTi film annealed at 500 °C.

For the PLD of $Ba_{0.80}$ $Sr_{0.20}TiO_3$, a krypton fluoride excimer laser (Lambda Physik COMPex 305) with a wavelength of 248 nm was used to deposit films of 400 nm. Pulsed laser deposition standard operation procedures are generally described elsewhere (Chang et al., 1999). The initial starting processing parameters included using a 1.5 cm x 1.5 cm platinum silicon wafer as a base substrate, background vacuum at 10^{-7} Torr, a 2.5-in sintered ceramic target of $Ba_{0.80}$ $Sr_{0.20}TiO_3$, an atmosphere of partial high-purity O_2 at 70 mTorr pressure, substrate temperature at 700°C, and laser beam energy density of 12.5 J/cm^2. A deposition of 30 minutes yielded a film thickness of 400 nm**.**

The final deposition technique for the piezoelectric films was metal organic solution deposition (MOSD). The advantage of MOSD processing includes low processing temperature, precise composition control, low equipment cost, and uniform deposition over large area substrates (Joshi et al 1998; Cole et al, 2000; Cole et al, 2001)**.** To fabricate these thin films, barium acetate, strontium

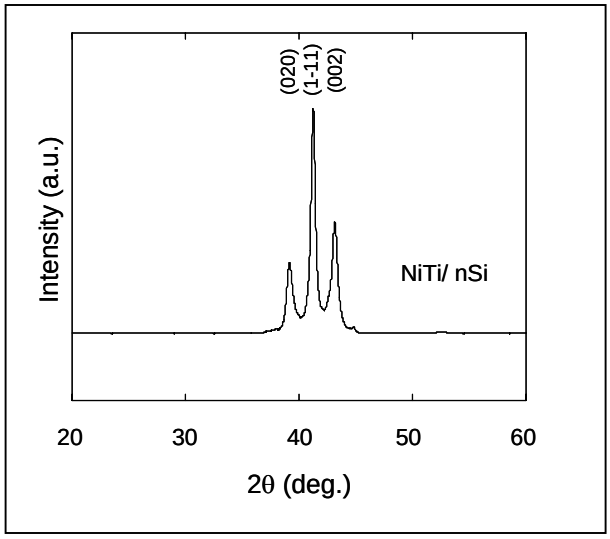

Figure 3. X-ray diffraction patterns of NiTi films deposited by DC magnetron in situ annealed at 500 °C.

acetate, and titanium isopropoxide were selected as precursors, and 2-methoxyethanol was chosen as solvents.

Barium acetate and strontium acetate were initially dissolved in glacial acetic acid. The clear solutions, thus formed, were added to the solution of titanium isopropoxide in 2-methoxyethanol (controls viscosity) to prepare a stoichiometric, clear, and stable BST precursor solution. The solution was spin-coated on Si substrates through 0.2 μm syringe filters. Five layer were deposited to achieve the desired thickness. Films were pyrolised at 350°C between spin coats. Glancing angle x- ray diffraction (GAXRD), using a Bruker D5005 diffractometer with CuKα radiation, was employed to assess film crystallinity. A Digital Instruments Dimension 3100 atomic force microscope (AFM) and a Hitachi S4700 field emission scanning electron microscope (FESEM) were utilized to assess film surface morphology and cross sectional microstructure, respectively.

3. RESULTS

In order to investigate the design and the materials selection for the vibration control, the configuration was measured against the existing, competing technology e.g. vicoelastic, which already has high material dispersion coefficient, tan δ, but low material stiffness and a narrow temperature range. It was imperative to identify various materials to determine the proper structure of the stack. Several modeling configurations were calculated and observed. Al_2O_3, Pb-Sn, Si, Pt, BST, SiO_2, and Ti were chosen for various vibration damping configuration pedestals. It was determined that the optimum pedestal design was a multilayered thin film composite with piezoelectric and shape memory alloy layers.

3.1 Model Development

To examine the insertion of a vibration control pedestal within the package between the ARS die and the base of the package, vibration modeling for a 1-D thin plate composite was developed. The pedestal was a multilayered thin film composite with piezoelectric, shape memory alloy, metal, and ceramic layers. A minimum of 50% reduction of incident energy was necessary to allow the MEMS ARS to operate effectively. To investigate this problem, a multilayered modeling approach was used. An incident compressional energy wave, I_0, entered the bottom of the pedestal from the package. At each interface within the composite, a certain amount of the incident energy, I_j, was reflected, R_j. Additionally, another packet of energy was viscously damped, and a final amount of incident energy was removed via piezoelectric (shape memory) loss mechanisms. The piezoelectric and viscous effects had a normal and shear component. The incident energy was assumed to be parallel to the normal of the pedestal.

A continuum mechanics model was used, and a 1-D infinite string assumption was made. Assuming that all of the incident and traveling waves are of the form $Fexp(-i\omega Z)$, which satisfies the wave equation; specifically, for a forced oscillator with the inclusions for internal damping. It is possible to imagine a 1-D wave traveling only in the longitudinal direction of the film with minimal interactions in the transverse directions. This is a reasonable assumption, as our materials have a thickness that is significantly less than the width, but it assumes that the shear components do not significantly contribute to the damping, which is not entirely accurate for piezoelectrics and SMAs. Beginning with the wave equation for a forced oscillator with damping, it is possible to solve for the 1-D wave equation. Once solved, determining the reflection and transmission coefficients is straightforward, and they are shown in Equations 1, 2, and 3, where k is a function of the input energy frequency (ω), the materials density (ρ) and modulus (τ)..

$$T = 1 - R = \frac{4k_1k_2}{(k_1 + k_2)^2}. \quad (1)$$

$$R = \left(\frac{k_1 - k_2}{k_1 + k_2}\right)^2. \quad (2)$$

$$\text{where } k \equiv \frac{\omega^2}{\upsilon^2} = \frac{\rho\omega^2}{\tau} \quad (3)$$

The critical thickness for damping at these frequencies is far larger than the thicknesses of the materials, leaving only the non-linear components (i.e. piezoelectric, piezomagnetic, or shaped memory) of the damped wave equation. Reflectivity and transmission are calculated at each interface, yielding a composite transmission model relating the input energy to the energy transmitted to the MEMS die. By examining the transmission of the energy through the composite structure, it is possible to see the effects of each layer. The energy enters the structure shown in Figure 1 and travels from the ceramic package to the lead-tin solder to the silicon wafer on the bottom as shown in Figure 2. The energy exiting the surface of the structure is the "final transmitted energy." The ratio of final energy to initial energy is the damping coefficient shown on the y axis of Figure 2. The layers that the energy passes through are listed on the x axis. Examining only the mechanical properties (i.e. reflection and transmission, etc.) and neglecting the non-linear damping components yields a structure that reduces the energy by less than 0.5% at steady state. When the "strain response" non-linear components are added for the barium titanate and the NiTi, over 45% of the initial input energy is damped. This damping can be increased to almost 90%, if the barium titanate and NiTi are deposited in such a way that a partial "phase change" occurs during transmission of the vibrational wave.

Based on the continuum modeling, three processing and stacking approaches for BST and NiTi were used to determine which stacking order is most appropriate for the passive damping vibration application. Various configuration of the films stack were experimented. The initial combination was with NiTi as a base layer and BST on top, then BST as the base layer via both PLD and MOSD and then, NiTi on top as the second layer of the pedestal. Details describe as follows.

3.2 Approach I

The first approach utilized NiTi as a base layer on Si wafer. Unlike their bulk counterparts, the as-deposited state of NiTi is amorphous. As such, an annealing step of temperatures of 500°C is required to cause grains to crystallize (Mohanchandra K. P et al, 2002). Figure 4a shows a dense cross-sectional structure; the BST MOSD was then deposited on top (Figure 4b). Since the MOSD films were annealed at elevated temperature (750°C), which is higher than the annealed temperature on NiTi itself, the Si and Ni inter-diffusion and react causing the inter surface to form nickel silicide, Ni_2S phase (Cole et al, 2000). Further investigation, such as electron diffraction, will determined the exact effect of the inter-diffusion. It is also not feasible to put NiTi as the bottom since BST is annealed at 750 ^{o}C

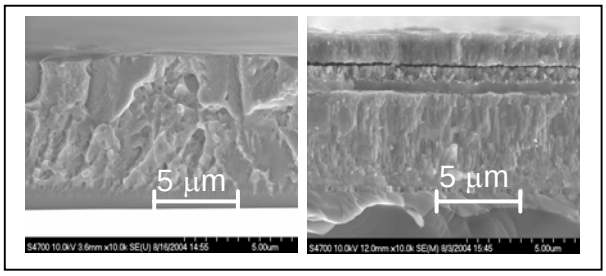

(a) (b)

Figure 4. Cross-sectional FESEM of (a) NiTi thin film on Si (b) bilayer of MOSD BST on top of NiTi.

which can cause the NiTi to react with Si. It is apparent that the piezoelectric should be the base layer of the bi-layer stack.

3.3 Approach II

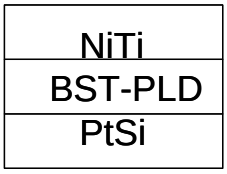

Pulsed laser deposition (PLD) was used to deposit a piezoelectric $Ba_{0.80}Sr_{0.20}TiO_3$, film on a Si wafer as a base layer. The as-deposited film was amorphous and required annealing at 750^{0}C to promote crystallinity (Cole et al, 2000; Cole et al, 2001, Joshi et al, 1998). Post deposition annealing was performed in a tube furnace in oxygen ambient for 60 minutes. The microstructure of the BST film exhibits a dense columnar grain structure as expected by physical vapor deposition (Chang et al, 2002, Ngo et al, 2002), the micrograph (figure 5a) indicates the surface morphology of the film is smooth with uniform large

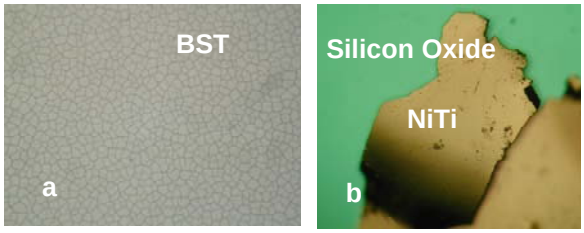

Figure 5. Plan view of (a) BST on PtSi (b) delamination of NiTi due to the high residual stress of BST film.

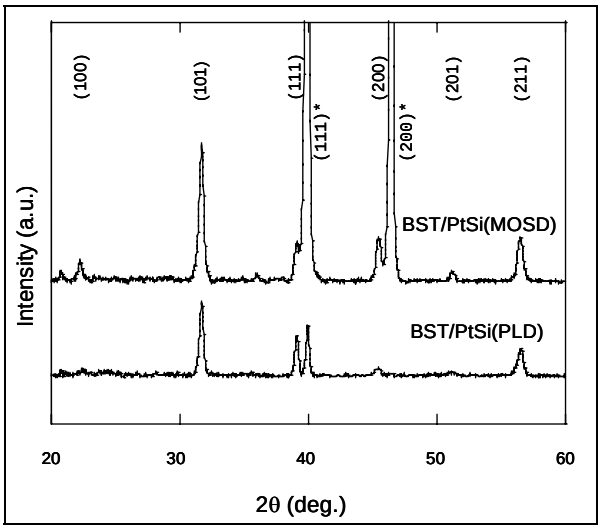

Figure 6. X-ray diffraction patterns of $Ba_{0.80}Sr_{0.20}TiO_3$ films deposited by PLD and MOSD post annealed at 750 °C.

domain like structure. Similar finding are also described elsewhere (Cole et al, 2000, Joshi et al 1998).

The GAXRD in Figure 6 also shows that the films exhibited a well-crystallized tetragonal phase at an annealing temperature of 750 °C. The NiTi film was then sputter deposited over both (1) the as-deposited and (2) annealed PLD piezoelectric films. However, this over-layer configuration was not successful. Specifically, after deposition of the NiTi film, the entire bi-layer stack delaminated from the Si support substrate (figure 5b). The lack of adhesion was found to be the result of the high residual stress (>750 MPa), which caused complete film delamination.

3.4 Approach III

The as-deposited MOSD fabricated film with NiTi over-layer also failed. This failure was attributed to the out-gassing of organic addenda from the MOSD processing, which resulted in a non-homogenous bilayer film stack.

However, the MOSD fabricated piezoelectric film, which was post deposition annealed prior to deposition of the NiTi over-layer, showed crystallized film after annealed (Figure 6). The results also agreed with previous findings (Cole et al, 2000; Cole et al, 2001). Roughness of the film also was a major consideration as the film surface must be coated with NiTi for this application. Good film to film adherence requires a smooth

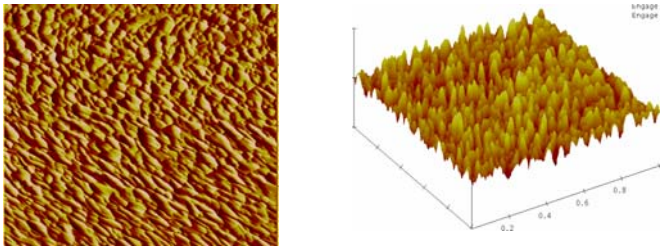

Figure 7. AFM of $Ba_{0.80}Sr_{0.20}TiO_3$ thin films. The scale bar indicates the vertical height. Surface roughness is 2.226 nm. Scan area is 1 μm^2.

defect free surface morphology. Quantitative analysis of the film surfaces determined the root-mean-square surface roughness, to be less than 2.2 nm for all MOSD films (figure 7). Surface roughness can be achieved as low as 1.2 nm by optimization of the processing procedure (Joshi et al, 2000). However, at the current roughness, the surface also is an extremely smooth films surface which is a major contribution to the excellent bonding with the NiTi in the bilayer stack pedestal. The images displayed in Figure 8 show the BST films exhibited a dense microstructure. The film also exhibits a uniform microstructure with an average grain size is around 50nm. It is critical to achieve uniform microstructure since it is an indication for fully crystallized and single phase film. A crystalline film is vital to ensure optimum and accurate damping properties, long term property reliability. This configuration resulted in a successful bilayer active thin film stack.

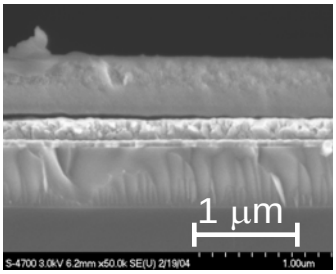

Figure 8. Cross-sectional FESEM of BST thin film deposited by MOSD.

CONCLUSION

Continuum mechanics modeling suggested that active materials, such as NiTi and piezoelectric films in a bilayer stack, employed in the design concept of the

passive vibration control pedestal is a reasonable approach to minimize the transmitted vibrations from the "external source" to the MEMS ARS. Shape memory alloy, NiTi, and piezoelectric, $Ba_{0.80}Sr_{0.20}TiO_3$ thin films were successfully deposited via DC sputtering process, PLD, and MOSD. The optimum pedestal designs consist of a 750 ^{0}C annealed MOSD fabricated BST film as the base layer and NiTi as the top layer of the bilayer structure. AFM characterization demonstrated that the resultant bilayer stacks has a surface roughness less than 2.2 nm and were crack and pinhole free. Cross-sectional microstructural and x-ray diffraction analyses showed the bilayer films to be dense and fully crystallized. Excellent surface morphological, microstructural, and structural properties of this bilayer stack demonstrated that the film processing methodologies employed resulted in an excellent bilayer active material stack suitable for the application of vibration damping. This performance achievement is essential to the realization of MEMS-based guidance in the next generation of U.S. Army munitions.

REFERENCES

Chang, W.; Horwitz, J. S.; Carter, A. C.; Kirchoefer, S. W.; Gilmore, C. M.; Chrisey, D. B., 1999: The Effect of Annealing on the Microwave Properties of $Ba_{0.5}$ $Sr_{0.5}$ TiO3 Thin Films, *Appl. Phys. Lett.*, 74, 7, 1003.

Chaplya, P. M. and Carman, G. P., 2002: Investigation of Energy Absorption Capabilities of Piezoelectric Ceramic, *J. Appl. Phys*., 92, 1504.

Cole, M. W.; Joshi, P. C.; Ervin, M. H., 2001: La Doped Ba_x $Sr_{1-x}TiO_3$ Thin Films for Tunable Device Applications, *Jour. Appl. Phys.*, 89, 6336.

Cole, M. W.; Joshi, P. C.; Ervin, M. H.; Hubbard C. Wood, M. C.; Pfeffer, R. L., Geil B.,2000: Improved Ni Based Composite Ohmic Contact to n-SiC for High Temperature and High Power Device Applications, *Jour. Appl. Phys.*, 88, 2655.

Cole, M. W.; Joshi, P. C.; Ervin, M. H.; Wood, M. C.; Pfeffer, R. L., 2000: The Influence of Mg Doping on the Materials Properties of BST Thin Films for Tunable Device Applications, *Thin Solid Films*, 374, 34.

Cole, M. W.; Nothwang, W.; Hirvonen, J.; Brown, G.; Carmen, G. P.; Mohanchandra, K.P., 2003: Harsh Environment Vibration Control for MEMS Inertial-Guidance Munitions: DARPA Proposal.

Cullity, B.D., 1978: *Elements of X-Ray Diffraction*, Addison-Wesley, 284.

Jeon Y. A., Choi E. S., Seo T.S, Yoon S.G: Improvements in Tunability of Barium Strontium Titanate Thin Films by Use of Metalorganic Chemical Vapor Deposited $BaSrRuO_3$ Interfacial Layers, *Appl. Phys. Lett.* 79(7), 1012.

Joshi, P. C. and Desu, S. B., 1998: Properties of $BaMg_{1/3}$ $Ta_{2/3}O_3$ Thin Films Prepared by Metalorganic Solution Deposition Technique for Microwave Applications, *Appl. Phys. Lett.* 73, 1080.

Kamalasanan, M. N. Chandra, S. Joshi, P. C.; Mansingh, Abhai; 1991: Structural and Optical Properties of Sol-gel-processed BaTiO, Ferroelectric Thin Films, *Appl. Phys. Lett*., 59(19), 4.

Mohanchandra K. P.; Ho K. K; and Carman G. P., 2002: Influence of Target Temperature on Sputter Deposited Ti-Ni-Cu and Ti-Ni-Pd Shape Memory Alloys, *Smart Structures and Materials*, 4699, 217.

Morita, T.; Wagatsuma, Y.; Cho, Y.; Morioka, H.; Funakubo, H.; 2004: Ferroelectric Properties of an Epitaxial Lead Zirconate Titanate Thin Film Deposited by a Hydrothermal Method Below the Curie Temperature *Appl. Phys. Lett*., 84, 5094.

Ngo, E.; Joshi, P. C.; Cole, M. W.; Hubbard, C., 2001: Electrophoretic Deposition of Barium Strontium Titanate Composite Thick Films for Microwave Application: *Appl. Phys. Lett*., 79, 248.

Singh P. K.; Cochrane S.; Liu W.T.; Chen K.; Knorr D. B.; Borrego J. M.; E. J. Rymaszewski E. J.; Lu T.M., 1995, High-Frequency Response of Capacitors Fabricated from Fine Grain BaTiO3Thin Films, *Appl. Phys. Lett*. 66 (26), 3683.

Woolman J.; Mohanchandra K.P.; Carman G. P.; 2003, Composition and Annealing Effects on the Mechanical Properties of Superelastic Thin Film Nickel Titanium, *Smart Structures and Materials*, 5053, 230.

….

FABRICATION OF ACTIVE THIN FILMS FOR VIBRATION DAMPING IN MEMS DEVICES FOR THE NEXT GENERATION ARMY MUNITION SYSTEMS

E. Ngo*, W. D. Nothwang, M.W. Cole, C. Hubbard, G. Hirsch,
D. Demaree, J. Hirvonen
U. S. Army Research Laboratory
Weapons and Materials Research Directorate
Aberdeen Proving Ground, MD 21005

K.P. Mohanchandra and G. P. Carman
Mechanical & Aerospace Engineering Department
University California at Los Angeles
Los Angeles, CA 90095-1361

Objective

To demonstrate a novel "Enabling Technology-Materials Solution", to allow propellant and/or gun-launched projectiles to achieve "required performance specifications" in harsh mechanical vibrations inherent to high-G forces and/or in flight environments. Fabricate individual layers of thin film NiTi and BST (80/20) on a variety of heterostructure bilayer material.

Potential Use:

Vibration damping across the full spectrum of guided munitions and/or any related commercial and military vibrating applications.

Outline

Objective

Background

- Existing Technology
- Problem
- Damping Approaches
- Materials Selection
- Technical Concept
- Design Concept

Experimental

- Continuum mechanics modeling
- Film Heterostructure Designs
- Film Heterostructure Down Selection
- Fabrication and Characterization

Summary and Conclusions

Abstract

OBJECTIVE:

This research combined continuum mechanics modeling, materials design, materials fabrication/processing, and experimental testing/characterization to promote a materials solution for passive damping of undesirable extrinsic vibrations in microelectromechanical - systems-based devices.

HOW:

Fabricate active/smart materials, i.e., piezoelectric [PZ] and shape memory alloy [SMA] thin films in an ARL design concept model, for passively damping spurious vibrations of device/die level structures that reduce the accuracy of MEMS inertial guidance systems.

24th Army Science Conference
email: engo@arl.army.mil

Existing Technology

MEMS-Based Inertial-Guidance Systems
MEMS navigational devices positioned into the control module of the missile system

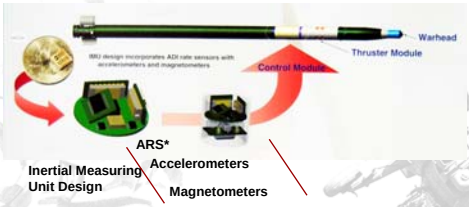

- **Guide projectiles (munitions/missiles) to their designated targets**
- **Derive positional information from measured acceleration and time data**
- **Angular Rate Sensor (ARS) work by measuring the relative motion of a resonating beam out from the plane of resonance (resonant frequency 8 kHz to 25 kHz). Motion is proportional to the angular rotation of the device and is sensed with respect to the package.**

MEMS-Based Inertial-Guidance Systems

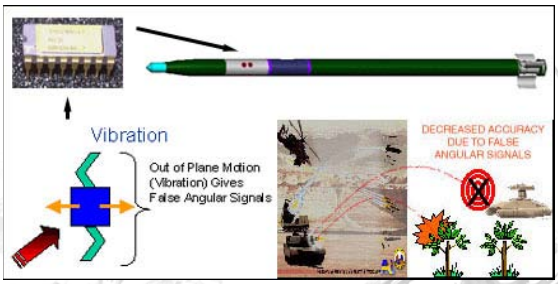

Concern

Since the MEMS-derived positional data is essential for the projectiles guidance/navigation, this false (out-of-plane motion), vibration-derived angular rate signal causes the projectile to miss its designated target. Thus, reduction of susceptibility of the MEMS ARS to the adverse extrinsic vibrations must be addressed to ensure the accuracy of positional performance (i.e., ensure target-hit success) for such gun launched projectiles

Background: MEMS-Based Inertial-Guidance Systems

Guided Munitions

Guidance and Navigation Essential
Inherent Harsh Mechanical Vibrations
Vibrational "Cross-Talk"
Enabling Technology

Vibration Mitigation Solution Criteria

High performance
Maintain System Performance
MEMS Scale
No Additional Power
Low cost
MILSPEC Standards
Foundry Friendly

Background Vibration Damping

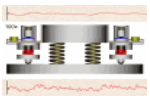

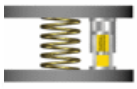

What is damping? **Damping is the energy dissipation properties of a material or system under cyclic stress.**

Vibration damping is when energies are damped when material absorbs external energy converts it to another form [heat, light work or stored energy]. The idea of vibration damping is to minimize amount of transmitted energy

(a) Active: sensors and actuators to attain vibration sensing - then suppress vibrations in real time

(b) Passive: Relies on materials inherent ability to absorb vibration energy by mechanical deformation thereby provides energy dissipation

Material Damping Effectiveness **FOM = (tan δ) • (M)**

Viscoelastic materials [VEMS] absorb energy due to polymer chain rotation/extension

Low stiffness
Thermal/moisture susceptibility
Frequency limitations

Background: Approach and Materials Selection

Passive Vibration Damping:

- Micro-Scale-Smart Material Approach – (**Thin Film)**
- Relies on **inherent non-linear deformations** produced when these materials are **mechanically loaded** [reversible process inherent to the materials]
- **Smart material** tuned to **absorb** the **external vibration** the system experiences
- **Composite** of smart material layers applicable across a **broad spectrum of vibration conditions**

Maximize the amount of energy damped

ARL CONCEPT- Micro/Nano Scale!!!!

- **High elastic modulus (M)**
- **High material dispersion coefficient (tan δ)**
- **Smart materials stiffness values orders of magnitude larger than VEMS**

ARL Design Concept: Vibration Control Pedestal

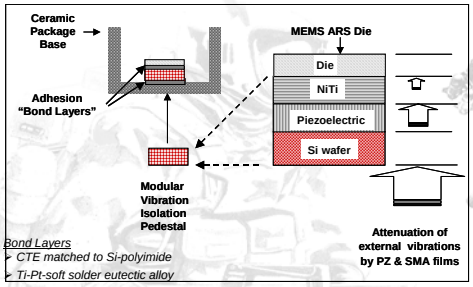

Integration of Vibration Control Pedestal at Die Level Within Ceramic Package

- **Minimum of increased effort**
- **Minimum additive process steps**
- **Minimum added device height**
- **Cost effective**

Modular pedestal applicable to a wide array of device structures with minimal modification of the die-package integration methodology

ARL Design Concept: Vibration Control Pedestal

Most Important Features of Design Concept:

- *Novel approach for damping MEMS-ARSs*
- *Unique damping treatment for a wide range of system/die level components*
- *Fabrication of smart/active vibration damping thin films on Si via low-cost processing methods*
- *Ease of pedestal integration within the MEMS package via foundry friendly processing*
- *Realization of pedestal integration without sacrifice of device performance*
- *Prototype vibration damping control pedestal will reduce external vibrations by at least 50%*
- *Modular die level design concept can be readily inserted into a variety of applications*
- *Foundry friendly process protocols will ensure technology transition to commercialization*

Modeling Efforts

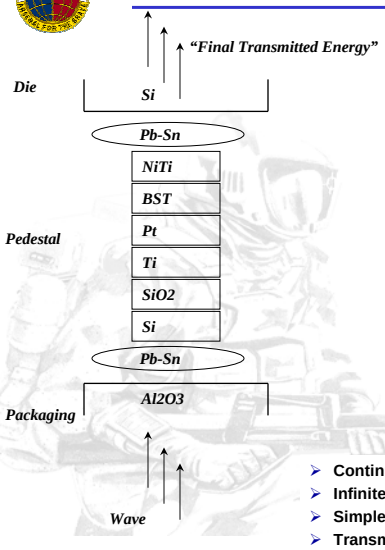

Reflection (R) and transmission (T) coefficients can be calculated by these equation where *k* is a function of the input energy frequency (ω), the materials density (ρ) and modulus (τ)..

$$T = 1 - R = \frac{4k_1k_2}{(k_1 + k_2)^2}$$

$$R = \left(\frac{k_1 - k_2}{k_1 + k_2}\right)^2$$

- **Continuum Model- longitudinal vib. mode**
- **Infinite String**
- **Simple "Dissipative" Strain Response**
- **Transmitted Waves**

ARL Design Concept: Modeling Efforts

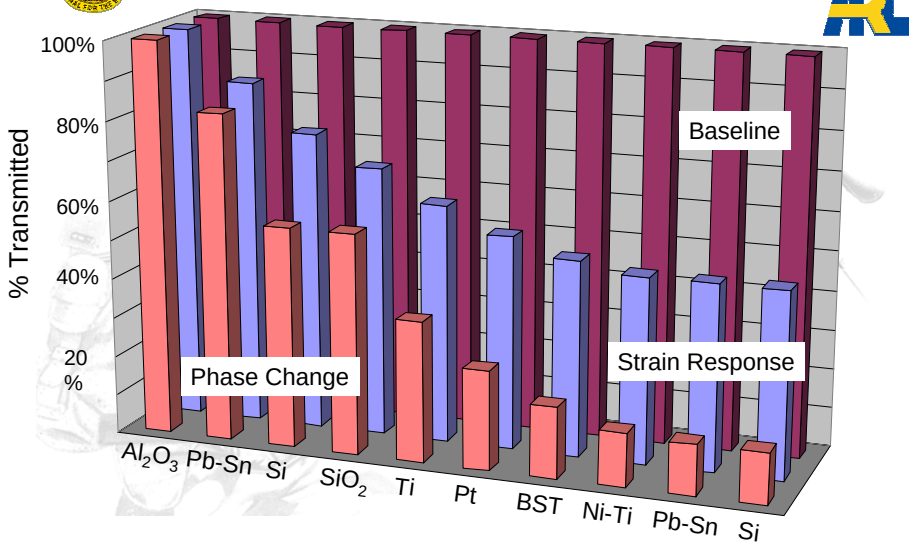

Experimental: Film Heterostructure Designs

Two Combinations Heterostructure Designs

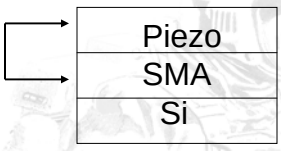

Piezo: $Ba_{0.80}Sr_{0.20}TiO_3$ → **MOSD**
→ **Pulsed Laser Deposition**

SMA: NiTi → **DC Sputter Deposited**

Thickness Limitations & Methodology

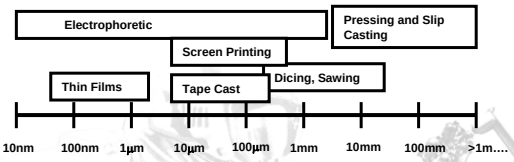

Quick comparison of thickness limitations and processing methods. Thin film has a narrower range of thickness compared to others technology but offers much more feasibility in system integration, light weight and can be economically mass produce.

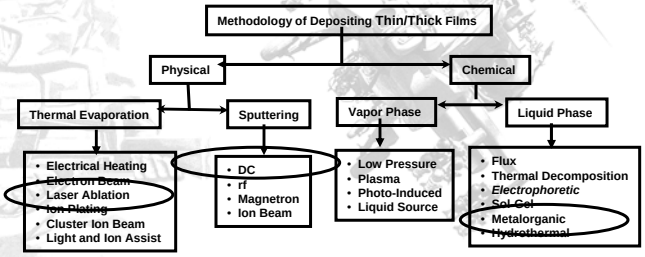

BST Film Fabrication Techniques

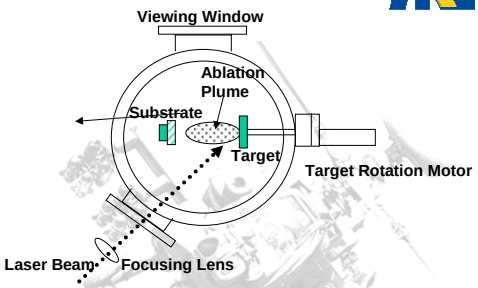

PLD PARAMETERS

- Lambda Physik Compex 305 excimer laser
- BST Film PLD from 99.9% pure target-*BST*
- Base pressure<1.0x10^{-6} Torr
- Beam focused on to rotating target with a 45° incident angle
- Sample-target separation 25 cm
- Laser fluence 12.1 Jcm^{-2}
- Ts= room temperature and 700 °C
- O_2 Partial Pressure 70 Mtorr
- Deposition Time 15 mln.

BST Film Fabrication Techniques

Parameters

Source : 3-inch DC magnetron gun
Base pressure: 5 x l0-8 Torr
Back Fill Gas: argon
Back Fill pressure:2 x l0-3 Torr
Target distance: 4 cm
Power: 300 Watts
Deposition Rate: 0.76 nm/s.
In-situ annealed: 500 °C for 10 min
Residual Gas Analyzer (RGA): contamination

NiTi [49:51] DC Sputtering Technique

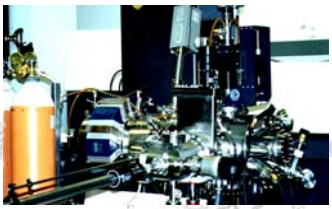

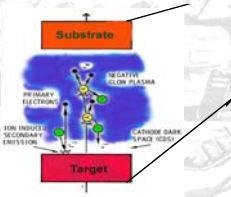

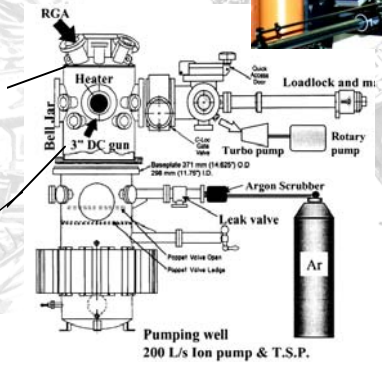

Metalorganic Solution Deposition Technique

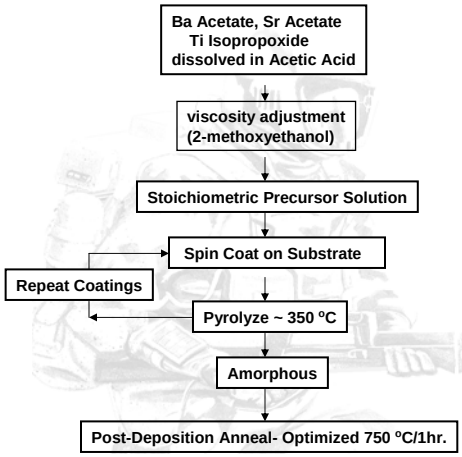

Advantage of MOSD

- **low processing temperature**
- **precise composition control**
- **low equipment cost**
- **uniform deposition over large area substrates**

Approaches

I	*II*	*III*
BST	NiTi	NiTi
NiTi	BST-PLD	BST-MOSD
Si	Si	Si

Experimental: Heterostructure Design Down-Selection

Optimize Films

NiTi
Si

- **XRD**
- **AFM**
- **FESEM**
- **RBS**
- **Auger**
- **EDS**

Bi-layer Design Film

BST
NiTi
Si

24th Army Science Conference
email: engo@arl.army.mil

Experimental: Heterostructure Design Down-Selection

Approach I.

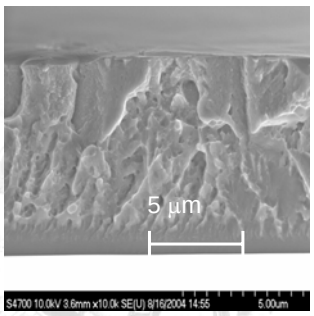

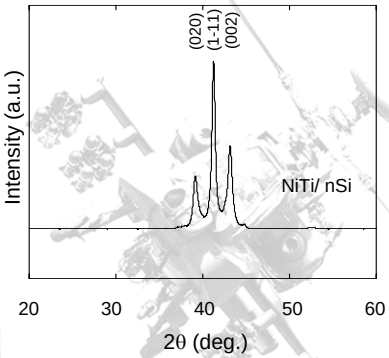

NiTi
Si

(a) Cross-sectional FESEM of NiTi thin film on Si (b) X-ray diffraction patterns of a well crystallized NiTi films deposited by DC magnetron in situ annealed at 500 °C.

Experimental: Heterostructure Design Down-Selection

BST / NiTi /Si Substrate

Bi-layer Design Film

BST
NiTi
Si

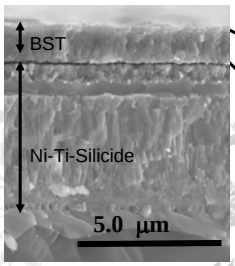

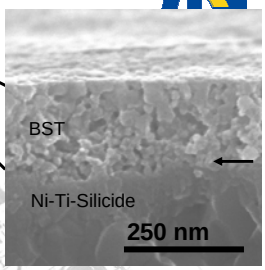

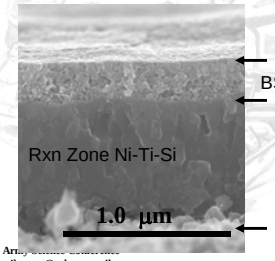

Post Anneal for NiTi T_p = 500 °C

Post Anneal for BST T_p = 750 °C

Ni-Ti-Si reaction zone Tp >>500 °C

Verified by XRD

Heterostructure design rejected

Experimental: Heterostructure Design Down-Selection

Approach II.

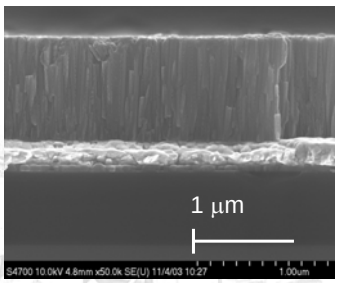

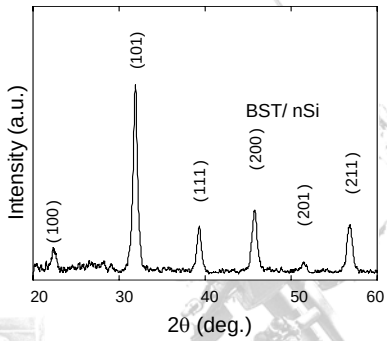

BST-PLD
Si

The microstructure of the BST film exhibits a dense columnar grain structure as expected. X-ray diffraction patterns of a well crystallized BST films deposited by PLD annealed at 750 °C.

Experimental: NiTi – BST [PLD]/Si Heterostructure

Approach II.

NiTi
BST-PLD
Si

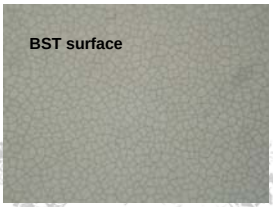

Plan-view image PLD deposited BST film

- **Large stress in PLD deposited BST film >750MPa**
- **Failure to adhere and delaminating of BST during NiTi deposition**
- **PLD Processing of BST rejected**

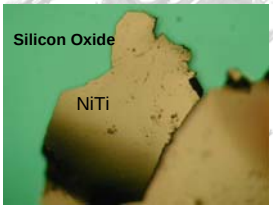

Plan-view image after NiTi film deposition

Experimental: NiTi – BST [MOSD]/ Si Heterostructure

Approach III.

NiTi DC Sputter, Ts=500 °C, anneal 500 °C/20 min

NiTi
BST-MOSD
Si

BST MOSD technique:

Annealed 750 °C/ 60 min prior to NiTi

Annealed 750 °C/ 60 min

Experimental: NiTi – BST [MOSD]/Si Heterostructure

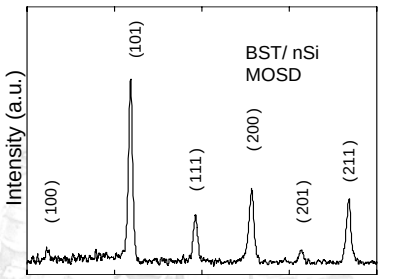

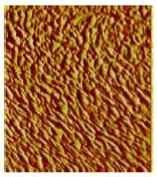

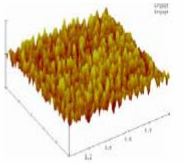

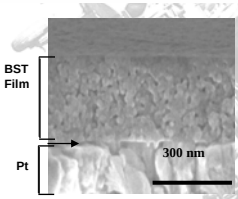

- Crystalline quality of the film improves with increasing annealing temperature
- No evidence of secondary phases
- Polycrystalline, no preferred orientation of films

Experimental: BST Annealing Optimization Composition and Interduffusion

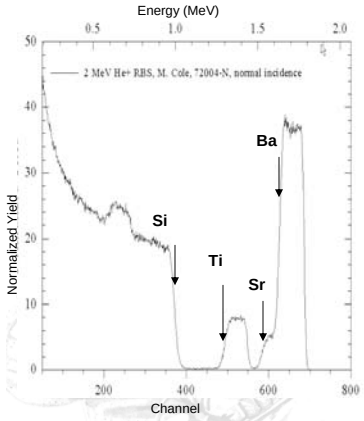

RBS Spectrum BST/Si substrate T_a=750 ºC

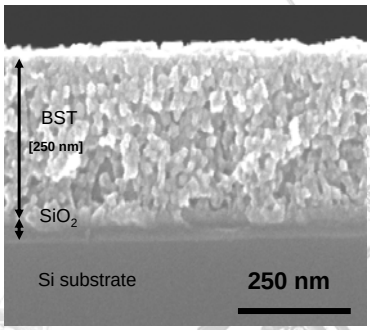

Sharp low energy edges of Ba, Sr, Ti peaks
Sharp high energy edge of Si signal
No evidence of interdiffusion BST-Si T_A=750 ºC
Ba:Sr 80:20
BST film ~250 nm thick

Summary and Conclusions

- **Continuum mechanics modeling suggested that NiTi and piezoelectric films in a bilayer stack, employed in the design concept of the passive vibration control pedestal is a reasonable approach to minimize the transmitted vibrations from the "external source" to the MEMS ARS.**
- ***Fabricated and down-selected two combination of heterostructure design concepts***
- ***Evaluated and down-selected materials process science for optimization of design concept***
- ***Successfully fabricated the smart/active vibration damping thin films on Si via low-cost processing methods***
- **Shape memory alloy, NiTi, and piezoelectric, Ba0.80Sr0.20TiO3 thin films were successfully deposited via DC sputtering process, PLD, and MOSD.**
- **Excellent surface morphological, microstructural, and structural properties of the ARL bilayer stack demonstrated that the film processing methodologies employed resulted in an excellent bilayer active material stack suitable for the application of vibration damping.**

Possible Future Efforts

- **Alternative substrate such as PtSi, Sapphire, SiC**
- **Investigate Bond Layers**
- **Evaluating adhesive bonding**
- ***Integrating and evaluating complete system***
- ***Prototyping***

References

Chang, W.; Horwitz, J. S.; Carter, A. C.; Kirchoefer, S. W.; Gilmore, C. M.; Chrisey, D. B., 1999: The Effect of Annealing on the Microwave Properties of Ba 0.5 Sr0.5 TiO3 Thin Films, *Appl. Phys. Lett.*, 74, 7, 1003.

Chaplya, P. M. and Carman, G. P., 2002: Investigation of Energy Absorption Capabilities of Piezoelectric Ceramic, *J. Appl. Phys*., 92, 1504.

Cole, M. W.; Joshi, P. C.; Ervin, M. H., 2001: La Doped Ba x Sr1-xTiO3 Thin Films for Tunable Device Applications, *Jour. Appl. Phys.*, 89, 6336.

Cole, M. W.; Joshi, P. C.; Ervin, M. H.; Hubbard C. Wood, M. C.; Pfeffer, R. L., Geil B.,2000: Improved Ni Based Composite Ohmic Contact to n-SiC for High Temperature and High Power Device Applications, *Jour. Appl. Phys*., 88, 2655.

Cole, M. W.; Joshi, P. C.; Ervin, M. H.; Wood, M. C.; Pfeffer, R. L., 2000: The Influence of Mg Doping on the Materials Properties of BST Thin Films for Tunable Device Applications, *Thin Solid Films*, 374, 34.

Cole, M. W.; Nothwang, W.; Hirvonen, J.; Brown, G.; Carmen, G. P.; Mohanchandra, K.P., 2003: Harsh Environment Vibration Control for MEMS Inertial-Guidance Munitions: DARPA Proposal. Cullity, B.D., 1978: *Elements of X-Ray Diffraction*, Addison-Wesley, 284.

Jeon Y. A., Choi E. S., Seo T.S, Yoon S.G: Improvements in Tunability of Barium Strontium Titanate Thin Films by Use of Metalorganic Chemical Vapor Deposited BaSrRuO3 Interfacial Layers, *Appl. Phys. Lett.* 79(7), 1012.

Joshi, P. C. and Desu, S. B., 1998: Properties of BaMg1/3 Ta2/3O3 Thin Films Prepared by Metalorganic Solution Deposition Technique for Microwave Applications, *Appl. Phys. Lett.* 73, 1080.

Kamalasanan, M. N. Chandra, S. Joshi, P. C.; Mansingh, Abhai; 1991: Structural and Optical Properties of Sol-gel-processed BaTiO, Ferroelectric Thin Films, *Appl. Phys. Lett*., 59(19), 4. Mohanchandra K. P.; Ho K. K; and Carman G. P., 2002: Influence of Target Temperature on Sputter Deposited Ti-Ni-Cu and Ti-Ni-Pd Shape Memory Alloys, *Smart Structures and Materials*, 4699, 217.

Morita, T.; Wagatsuma, Y.; Cho, Y.; Morioka, H.; Funakubo, H.; 2004: Ferroelectric Properties of an Epitaxial Lead Zirconate Titanate Thin Film Deposited by a Hydrothermal Method Below the Curie Temperature *Appl. Phys. Lett*., 84, 5094.

Ngo, E.; Joshi, P. C.; Cole, M. W.; Hubbard, C., 2001: Electrophoretic Deposition of Barium Strontium Titanate Composite Thick Films for Microwave Application: *Appl. Phys. Lett*., 79, 248. Singh P. K.; Cochrane S.; Liu W.T.; Chen K.; Knorr D. B.; Borrego J. M.; E. J. Rymaszewski E. J.; Lu T.M., 1995, High-Frequency Response of Capacitors Fabricated from Fine Grain BaTiO3Thin Films, *Appl. Phys. Lett*. 66 (26), 3683.

Woolman J.; Mohanchandra K.P.; Carman G. P.; 2003, Composition and Annealing Effects on the Mechanical Properties of Superelastic Thin Film Nickel Titanium, *Smart Structures and Materials*, 5053, 230.

24th Army Science Conference
email: engo@arl.army.mil